Available online at www.sciencedirect.com
SCIENCE DIRECT®
Sensors and Actuators A 114 (2004) 135–140
SENSORS AND ACTUATORS A PHYSICAL
www.elsevier.com/locate/sna

AFM characterization of out-of-plane high frequency microresonators☆

Steve Ryder, Ki Bang Lee*, Xiaofan Meng, Liwei Lin

Department of Mechanical Engineering, Berkeley Sensor and Actuator Center, University of California at Berkeley, 1113 Etcheverry Hall, Berkeley, CA 94720-1740, USA

Received 1 July 2003; received in revised form 9 December 2003; accepted 16 December 2003

Available online 3 March 2004

Abstract

The feasibility of characterization of vertically driven high frequency microresonators using atomic force microscopy (AFM) has been successfully demonstrated to easily measure resonant frequency of high frequency resonator. The distinctive achievement of this technique is the rapid, direct characterization of resonant frequency and quality factor for structures that cannot be readily characterized using optical or electrical techniques. Experimentally, an annular high frequency resonator was measured to have its fundamental resonance mode at 2.75 MHz with a quality factor of 6. Discrepancy between design and measured frequency is due to fabrication process errors and dynamic coupling error. This new characterization approach might be a good candidate for easy detection of high frequency microresonators.

Keywords: Characterization; High frequency; RF MEMS; AFM; Microresonator; Microsystems

1. Introduction

Characterization of high frequency MEMS resonators is often the most challenging stage in their design cycle. As frequency scales, the magnitude of resonant response decreases correspondingly. Direct optical observation under an optical microscope fails to identify the tiny movement of mechanical resonance at high frequency. If the device is characterized under scanning electron microscope (SEM), the trade-off between image resolution and image refresh rate becomes problematic. Detecting the tell-tale blur of a resonating structure requires a sharp image, which in turn is more difficult to obtain as the device feature size and vibration amplitude decreases. Furthermore, this highly inefficient process is even more difficult for the characterization of out-of-plane resonators.

Interferometry is well suited for out-of-plane resonator characterization, but the technology is not yet suitable for high frequency microresonators operating in the high-MHz and GHz ranges [1]. Commercially available laser Doppler vibrometry (LDV) systems can measure macroscale structures vibrating at up to 20 MHz, but the equipment available to measure microscale devices such as MEMS resonators is currently limited to a vibration frequency of 1 MHz. These LDV systems require microscopes to focus the laser beam to a spot size (1 μm) suitable to resolve the details of a vibrating MEMS structure. Electrical detection using capacitance or transconductance [2] often requires sophisticated electronics to boost signal-to-noise ratio and to avoid the interference of parasitic capacitances. As device frequencies scale up, the capacitive gap required to detect a signal also decreases. For some device architectures, the gap requirement strains the limits of IC fabrication. In this paper, atomic force microscopy (AFM) characterization is explored to measure resonant frequency of a high frequency microresonators for applications such as microresonator-based wireless communication systems.

2. AFM method

As an alternative to electrical characterization, we propose a direct, mechanical method using contact-mode AFM for in situ characterization of out-of-plane MEMS resonators. This method allows for the rapid detection of the device resonant frequency when other methods are ineffective or undesirable. AFM involves an atomically sharp probe tip affixed to a cantilevered beam which is raster scanned in close proximity over the surface of interest. Piezoactuators and feedback circuitry maintain a constant level of atomic force between the tip and the surface. The tip deflection is measured by reflecting a laser off the cantilever into a photo-detector. The

☆ A portion of this paper was presented at the 12th International Conference on Solid-State Sensors and Actuators (Transducers'03), 8–12 June 2003, Boston, USA.

* Corresponding author. Tel.: +1-510-642-8983.
E-mail address: kblee@me.berkeley.edu (K.B. Lee).

0924-4247/$ – see front matter © 2004 Elsevier B.V. All rights reserved.
doi:10.1016/j.sna.2003.12.033

deflection data is displayed as a topological relief map of the structure. This resulting image is formed line by line as the tip scans from side to side and top to bottom of its range. Since the AFM tip has a vertical resolution on the order of 1 nm or below, it is ideally suited for detecting extremely low-amplitude vibrations. The lateral resolution of the AFM measurements can be less than 25 nm due to the very fine AFM tip. Furthermore, with proper experimental setup, the mode shapes of vibrating micromechanical structures can be detected.

Experimentally, the sample is first scanned in an unactuated state. The scan is repeated, but now changing the actuation frequency every 5 or 10 scan lines. When the structure is being actuated near resonance, the change in structural displacement is immediately evident. Post-processing allows a comparison between actuated and unactuated states. In the Topometrix system used in this work, this entailed three-point leveling of the raw AFM data followed by measuring the topological data along vertical lines. It should be noted that, manually leveling the data is not a precise operation, requiring the judgment of the operator as to which three points will allow for good leveling. Thus the leveling process will introduce a certain amount of "noise" or variability into the results, even when working with the same data set. This method exploits the dynamics of the AFM cantilever so as to only measure vibrational amplitudes at resonance. Typical AFM cantilevers have natural frequencies in the kilohertz range. For structures vibrating at frequencies exceeding the bandwidth of the cantilever, the tip cannot track their motion and remains fixed at the structure's vibrational amplitude as it scans over the surface, as shown in Fig. 1, allowing the characterization of extremely high frequency resonators. Furthermore, AFM offers nanometer precision for out-of-plane deflection as well as spatial resolution such that the frequency spectrum of any part of the microresonator can be measured and the whole mechanical mode shape can be reconstructed afterwards.

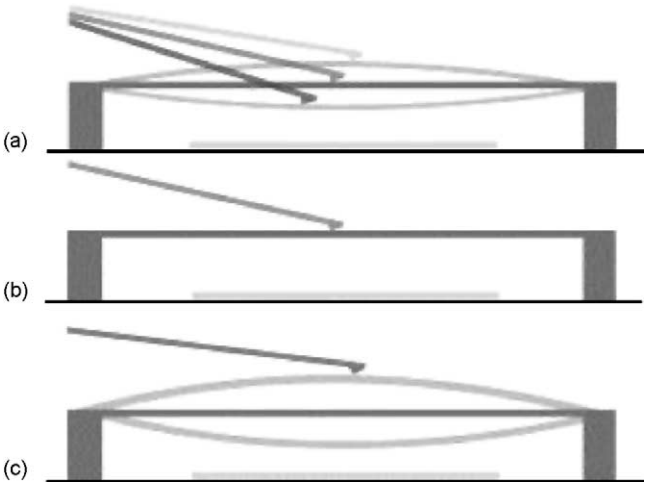

Fig. 1. AFM measurement of a resonator: (a) at low frequency, the cantilever tip can track the surface of the structure as it vibrates. At high but non-resonant frequencies, the amplitude of vibration is extremely small and cantilever remains stationary, as shown (b). At resonance (c), the structure is vibrating much faster than the natural frequency of the cantilever. The tip cannot follow the structure's surface and remains fixed at the maximum amplitude of vibration.

3. Design and fabrication

This technique was applied to an annular microresonator fabricated by a standard surface-micromachining process as shown with mode shape in Fig. 2 and SEM in Fig. 5 [3]. The inner and outer edges of the annulus are constrained as shown in Fig. 2, [5] resulting in a stiff structure with high natural frequency and very small vertical deflections. The governing equation for the resonant frequency of a fixed-fixed annulus is given by [4]:

$$f = \frac{\lambda_{ij}^2 h}{2\pi a^2}\sqrt{\frac{E}{12\rho(1-\nu^2)}} \quad (1)$$

where λ_{ij}^2, a, h, E, ρ and ν are the resonant frequency coefficient of the fixed-fixed annular structure, the outer radius of the annular structure, the thickness, Young's modulus, the density, and Poisson's ratio of the annular structure, respectively [4]. This theoretical calculation predicted a fundamental resonant frequency of 15.6 MHz for a fabricated and tested structure with $\lambda_{00} = 15.75$, $h = 1.5\,\mu\text{m}$ $\rho = 2330\,\text{kg/m}^3$, $E = 150\,\text{GPa}$ and $\nu = 0.29$. A design chart for these values, along with the ratio of the inner radius to the outer radius of the annular structure, $b/a = 0.7$, is shown below in Fig. 3. From this chart, the device was sized to have a fundamental resonant frequency of 15.6 MHz, with corresponding dimensions of $a = 96\,\mu\text{m}$, $b = 67\,\mu\text{m}$. The device was fabricated using the MUMPs process [3].

The process flow for these devices is shown below in Fig. 4. The process starts with the growth of a 0.6 μm

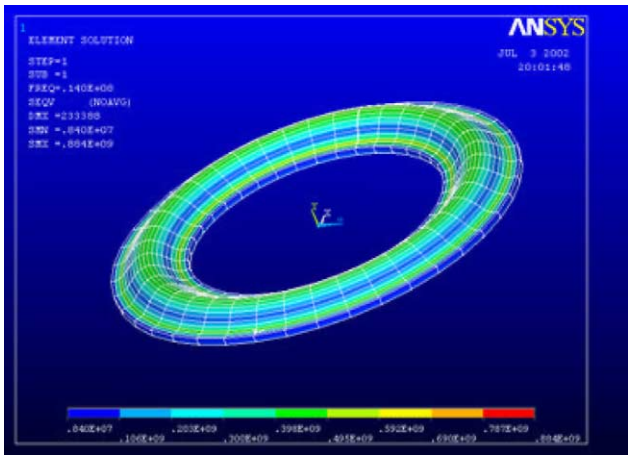

Fig. 2. Finite element analysis simulation results showing the first mode shape of the fixed-fixed annular structure with a predicted resonant frequency of 14.0 MHz.

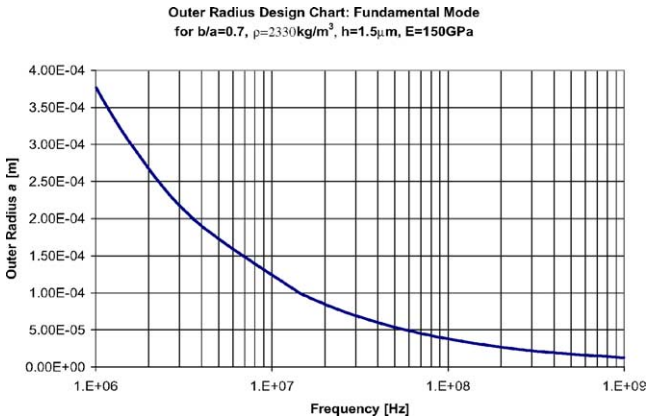

Fig. 3. Resonator design: outer radius is calculated for the first vibration mode of the fixed-fixed annular structure.

-thick, low stress lpcvd (low pressure chemical vapor deposition) silicon nitride layer on the silicon substrate as an electric isolation layer. In the processing step of Fig. 4(a), a 0.5 μm-thick LPCVD polysilicon (poly0) is deposited and patterned for the sensing and actuation electrode. A 2 μm-thick sacrificial PSG (phosphosilicate glass) layer is deposited in the step of Fig. 4(b). Fig. 4(c) shows that a 3.5 μm-thick polysilicon (poly1 and poly2) is deposited and patterned for constructing the annular structure. Both polysilicon layers should be used for maximal natural frequency, however, in the tested devices, only the 1.5 μm poly1 layer was used. Afterwards, a 0.5 μm-thick gold layer is deposited and patterned using lift-off to form the contact pads. The annular structure is released by etching the sacrificial PSG layer through the side etch holes (shown in Fig. 5) with hydrofluoric acid, followed by rinsing and drying the wafer. The final, released structure is shown in Fig. 4(d). Fig. 5 shows an SEM image of the fabricated resonator with a diameter 192 μm, which is designed with an annular structure to obtain a high resonant frequency. Several etch holes are used to remove the sacrificial PSG under the fixed-fixed annular structure. Fig. 6 shows the cross-sectional view of plane, A–A, in Fig. 5. In Fig. 6, input signal and AFM tip is placed for further explanation. The annular structure with the radius of a, the inner radius

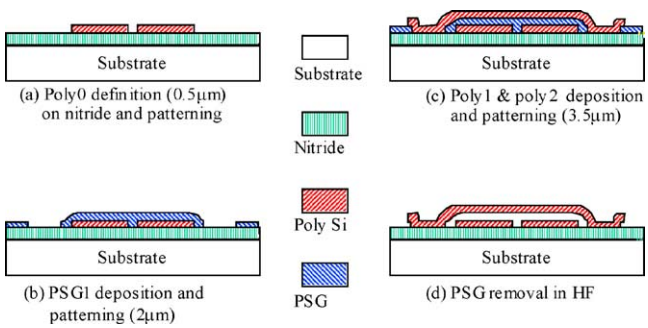

Fig. 4. Fabrication process for the annular high frequency resonator.

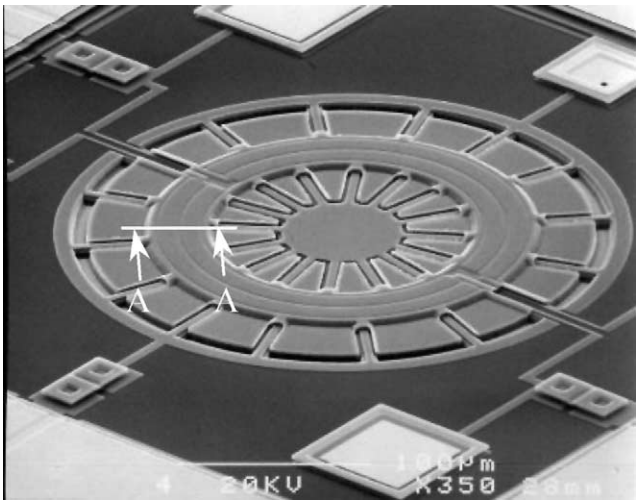

Fig. 5. An SEM image of the fabricated resonator with a diameter 192 μm. The resonator is designed with an annular structure to obtain a high resonant frequency. The cross-sectional view of the plane, A–A, is shown in Fig. 6.

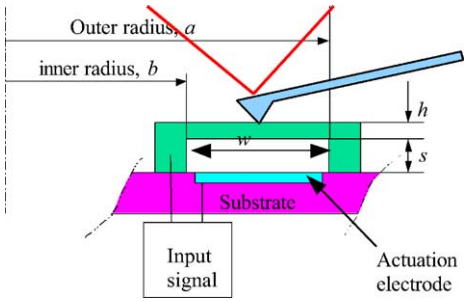

Fig. 6. Cross-sectional view of plane, A–A, in Fig. 5: The input signal actuates the fixed-fixed structure of the annular resonator while the AFM tip scans across the top surface, capturing the vibrational amplitude. In the fabricated structure, the nominal dimensions are: $a = 96\,\mu m$, $b = 67\,\mu m$, $h = 1.5\,\mu m$ and $s = 2\,\mu m$.

of b, and thickness of h is anchored and spaced by the space of s on the substrate.

4. Experiment

The AFM technique was employed specifically to counter the difficulties in characterizing this structure. Electrical detection fails because the 2 μm capacitive gap between the sensor electrode and the vibrating surface coupled with vibration amplitude of less than 200 nm, which cannot produce a detectable signal. Optical methods are similarly stymied by the device's high frequency of more than 1 MHz and low-amplitude out-of-plane vibrations. The microresonator was actuated with a 10 V peak-to-peak ac signal and a dc bias of 5 V in Fig. 6. The AFM is not capable of measuring the displacement of a single, fixed point, since it must raster scan to produce an image. Therefore, the minimum-sized region (5 μm × 5 μm) was scanned in order to approximate a

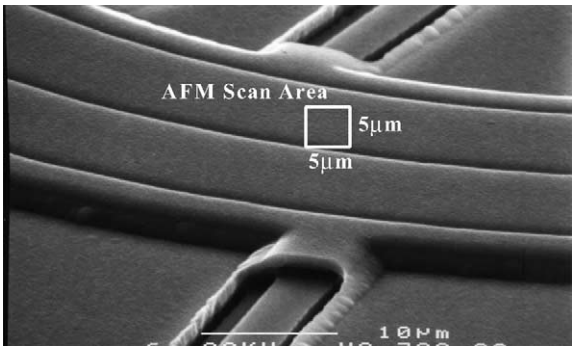

Fig. 7. SEM detail showing approximate 5 μm × 5 μm AFM scan region location and structural etch-hole features.

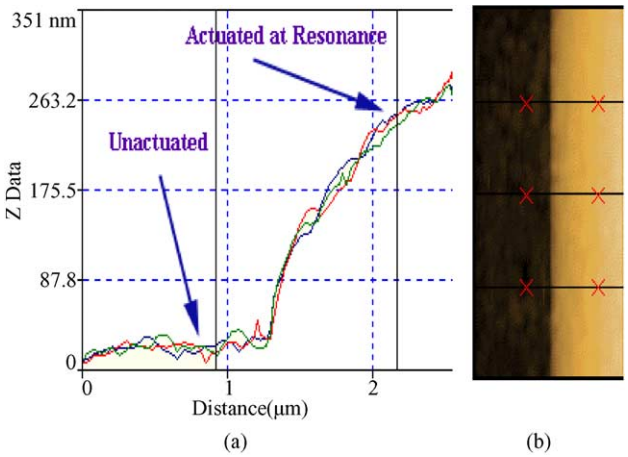

Fig. 8. AFM surface topographical data at resonance. The surface has a base height of around 40 nm when there is a dc but no ac signal. When the signal is applied at the resonant frequency, the AFM detects vibrations with displacements near 260 nm. (b) shows the two-D topology map over the same interval, with the dark and light bands representing the unactuated and actuated regions, respectively.

single point measurement, as shown in Fig. 7. Fig. 8 shows the clear distinction between the structural response of the unactuated and actuated structure as it is scanned from the edge of the structure toward the center.

The reconstructed amplitude versus frequency spectrum in Fig. 9 shows the natural frequency at 2.75 MHz with a quality factor (under atmospheric pressure) of 6. It should be noted that constructing frequency spectra using this method requires measuring the displacement of the actuated device relative to the unactuated state at each frequency. The AFM method excels in its ability to find quickly the resonant frequency of a device. Full characterization mitigates this advantage.

5. Discussion

It is noted that the measured resonant frequency of the device was less than 3 MHz, far below the value predicted by either theory or simulation. Such degradation can be

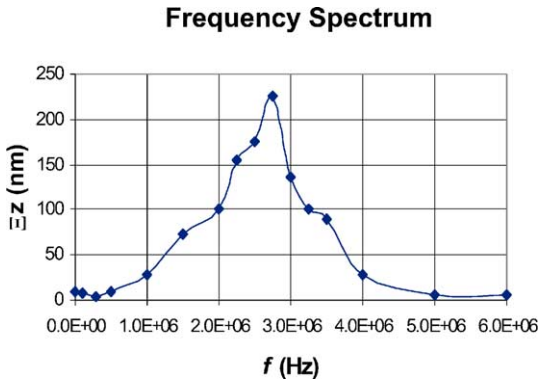

Fig. 9. Measured frequency spectrum of the annular micro-resonator. Data similar to that shown in Fig. 8 was collected over a wide range of frequencies and clearly shows a resonant response around 2.75 MHz with a Q (under atmospheric pressure) of roughly 6.

expected. First, the theoretical natural frequency is 11% higher than the simulated result because the theoretical model is based on a simple two-dimensional annulus fixed at both boundaries. In the simulation, the annulus is constrained with added anchors for better emulation of the real surface-micromachined structure. This additional degree of freedom will lower the natural frequency. Moreover, both theoretical calculations and finite element simulations are based on nominal structural parameters provided from the original design values. Actual dimensions are subject to fabrication variations. For example, in this foundry process [6], the structural thickness can be within the range of 1.5 ± 0.1 μm. If the thickness takes its worst-case value (e.g. 1.4 μm), the theoretical resonant frequency drops by 1 MHz. Another design and fabrication variation comes from that the original design placed two electrodes, one for driving and the other for sensing, under the annulus [3] by using the first polysilicon layer that is attached to the substrate. As a result, three “grooves” representing the shape of the two electrodes can be clearly observed for the annulus in Fig. 5. This effectively changes the flat annulus to a corrugated one and again, the real fundamental frequency is expected to drop. In the experiment, these two electrodes were tied together electrically to provide a larger actuation area. Other uncertainties could also affect the performance of the device, such as uncertain material properties and the effects of residual stress. For example, the process documentation from the foundry service specifies that the structural polysilicon layer has a residual compressive stress between 0 and 20 MPa, with the typical value falling midway between the two. Compressive stress generally decreases the value of resonant frequency as compared with the structures with zero stress used in the theoretical analyses. Furthermore, there are etching holes at the annulus boundary that provide extra freedom to the structure and further reduce the actual natural frequency.

Another important issue is to examine the dynamics that this method exploits. In principle, when the actuation

frequency greatly exceeds the bandwidth of the cantilever, the cantilever can no longer track the motion of the resonator, and the cantilever remains fixed at the position defined by the amplitude of the resonator's motion. Since the cantilever is not moving with the resonator, there should be very little dynamic coupling in terms of added mass and spring stiffness. Although sophisticated treatments of the complex dynamics of the AFM system exist in the literature (see [7–11]), in this work, the cantilever and the resonator are modeled as a simple lumped parameter spring-mass system, neglecting damping both internally in the cantilever and externally in the fluid that the AFM is operating in (air). In the worst-case scenario (with regard to dynamic coupling), which can occur at frequencies below the cantilever's bandwidth, the cantilever rests upon the structure's surface throughout the course of its motion. In this case, it is assumed that the AFM feedback control system can maintain contact between the tip of the AFM and the microresonator and that there is no nonlinear spring effect between them. Fig. 10 shows that (a) and (b) are one-degree-of-freedom models of the high frequency resonator and AFM cantilever and (c) is a lumped mass model when AMF tip directly contact the resonator. With these assumptions, the two masses would be coupled as shown in Fig. 10(c) and the new system's resonant frequency would be of the form:

$$f = \sqrt{\frac{k_\mathrm{r} + k_\mathrm{c}}{m_\mathrm{r} + m_\mathrm{c}}} \tag{2}$$

where the subscripts r and c denote the resonator and cantilever, respectively. m_r, m_c, k_r and k_c are the effective mass and stiffness of the resonator and AFM cantilever, respectively. We do not know how much the high frequency resonator and the cantilever of AFM is coupled and how much area is coupled with the AFM tip on the AMF cantilever. To briefly examine the resonant frequency degradation, we use the approximate data of mass and stiffness: (1) $m_1 = 1.38 \times 10^{-13}$ kg and $k_1 = 1328$ N/m of coupled width (in the circumferential direction) of 4 μm of the fixed-fixed resonator in Figs. 5 and 6 as the first order approximation and (2) $m_2 = 5.6 \times 10^{-12}$ kg and $k_2 = 0.064$ N/m from the tip and cantilever data (Topometrix Model No. 1520–00). In this case, Eq. (2) provides the estimated resonant frequency of 2.4 MHz that is comparable with the measured resonant frequency of 2.75 MHz from Fig. 9. It is noted from this simple estimation that the resonator and AFM cantilever are highly coupled to reduce the resonant frequency. The exact coupled mass m_1 and stiffness k_1 could not be obtained because we do not know the exact coupling mechanism. In the future, the coupling mechanism will be studied for better characterization. Table 1 summarizes possible errors in measurement of frequencies of the resonator. After reducing the coupling between the AFM and resonator, the AFM characterization could be used to characterize dynamic behavior of microresonator. The quality factor in Fig. 9 was measured as 6. The quality factor is low due to air damping between the resonator structure and the actuating electrode. A vacuum chamber or package could be used to get higher quality factor.

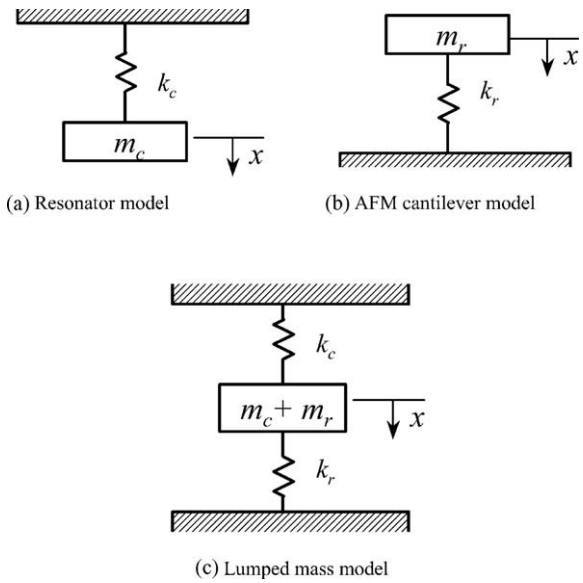

Fig. 10. (a) Resonator model (b) AFM cantilever model, and (c) lumped mass model. Lumped parameter spring-mass model of resonator and cantilever when the masses are directly coupled: (a) and (b) are one-degree-of-freedom models of the high frequency resonator and AFM cantilever, respectively; (c) lumped mass model when AFM tip directly contacts the resonator.

Table 1
Comparison of errors in resonant frequency

Resonant frequency (MHz)		Possible errors (MHz)	
Design	Measured	Thickness	Dynamic coupling[a]
15.6	2.75	±1	13.2

[a] Based on the assumed coupled resonator width of 4 μm in circumferential direction.

6. Conclusion

Direct AFM characterization of out-of-plane fixed-fixed high frequency microresonators is examined to measure resonant frequency. Contact-mode of AFM was used to measure the first mode resonant frequency of the high frequency resonator in the out-of-plane direction. The first mode resonant frequency and quality factor was measured as 2.75 MHz and 6 from experimental data, respectively. Discrepancy between measured and design data was observed mainly due to dimensional error from the fabrication process and dynamic coupling between the resonator and AFM cantilever. After reducing the coupling between the AFM and microresonator, AFM characterization of dynamic behavior of microstructures could be used to detect the resonant frequencies and mode shapes.

Acknowledgements

The authors would like to thank Dr. Bill Flounders and Mr. Michael Young at the Berkeley Sensor and Actuator Center (BSAC) for valuable discussions. Mr. Ryder is supported in part by a NDSEG Fellowship.

References

[1] C. Rembe, R.S. Muller, Measurement system for full three-dimensional motion characterization of MEMS, J. Microelectromech. Syst. 11 (5) (2002) 479–488.
[2] C.T.C. Nguyen, Frequency-selective MEMS for miniaturized low-power communication devices, IEEE Trans. Microwave Theory Tech. 47 (8) (1999) 1486–1503.
[3] K.B. Lee, S. Ryder, L. Lin, Design fabrication of an annular high frequency resonator, in: Proceeding of 2002 ASME International Mechanical Engineering Congress and Exposition, 17–22 November 2002, New Orleans, Louisiana, Paper #IMECE2002-33387.
[4] R.D. Blevins, Formulas for Natural Frequency and Mode Shape, Van Nostrand Reinhold Company, 1979.
[5] ANSYS Version 5.7, ANSYS Inc., Southpointe, Canonsburg, PA.
[6] D.A. Koester, R. Mahadevan, B. Hardy, K. Markus, MUMPs Design Handbook, Cronos Integrated Microsystems, Rev. 7, 2001.
[7] H. Safar, R.N. Kleiman, B.P. Barber, P.L. Gammel, J. Pastalan, H. Huggins, L. Fetter, R. Miller, Imaging of acoustic fields in bulk acoustic-wave thin-film resonators, Appl. Phys. Lett. 77 (1) (2000) 136–138.
[8] S. Salapaka, M.V. Salapaka, M. Dahleh, I. Mezic, Complex dynamics of repeated impact oscillators, in: Proceedings of the 37th IEEE Conference on Decision and Control, vol. 2, Tampa, Florida, December 1998, pp. 2053–2058.
[9] M. Ashhab, M.V. Salapaka, M. Dahleh, I. Mezic, Dynamical analysis and control of microcantilevers, Automatica 35 (1999) 1663–1670.
[10] J.M. Neumeister, W.A. Ducker, Lateral, normal, and longitudinal spring constants of atomic force microscopy cantilevers, Rev. Sci. Instrum. 65 (8) (1994) 2527–2531.
[11] S. Hirsekorn, U. Rabe, W. Arnold, Theoretical description of the transfer of vibrations from a sample to the cantilever of an atomic force microscope, Nanotechnology 8 (1997) 57–66.

Biographies

Steve Ryder joined the Mechanical Engineering Department at UC Berkeley in the fall of 2001 after graduating with his BS from Lafayette College in Easton, PA. His research activities have been primarily related to the characterization and optimization of microresonators. He received his Master's degree in 2003.

Ki Bang Lee received the BS, MS, and PhD degrees, all in mechanical engineering, from the Hanyang University, Seoul, Korea, and the Korea Advanced Institute of Science and Technology (KAIST), Korea, in 1985, 1987, and 2000, respectively. He worked on MEMS and vibration projects with Samsung Advanced Institute of Technology (SAIT), Yonginsi, Korea during 1987–2000, holding the last position of principal research scientist. He was a post-doctoral researcher at Berkeley Sensors and Actuator Center (BSAC) at the University of California at Berkeley during 2000–2003. As a research specialist, he has worked on a MEMS project with Professor Albert P. Pisano at BSAC since 2003. His research interests include design and fabrication of microsensors/microactuators, including microgyroscope and frequency/quality-factor-tunable microactuators; microbatteries and micropower generation; optical microsystems on a chip; integrated disposable microsystems such as DNA chip or labs-on-a-chip with disposable micropower; microvehicles for MEMS/bioMEMS application; microfluidic devices; and MEMS packaging. He has been granted eight US patents in the area of MEMS and four Korean patents in the area of MEMS and ink-jet technology.

Xiaofan Meng is senior development engineer in Department of Electrical Engineering and Computer Sciences, UC Berkeley. He received the BS degree in physics in 1964, the PhD degree (equivalent) in physics in 1976 from Department of Physics, Peking University. He was assistant and associate professor at Department of Physics, Peking University and became The director of Superconducting Electronics Group from 1984. Since 1987 he was visiting professor at Department of Electrical Engineering and Department of Physics, University of Virginia. From 1991 he became visiting research scientist in Department of Electrical Engineering and Computer Sciences, UC Berkeley. His current research interests include superconductor, semiconductor and MEMS device and IC process development.

Liwei Lin (September'92–March'93) received the MS and PhD degrees in mechanical engineering from the University of California, Berkeley, in 1991 and 1993, respectively. From 1993 to 1994, he was with BEI Electronics, Inc., USA, in research and development of microsensors. From 1994 to 1996, he was an associate professor in the Institute of Applied Mechanics, National Taiwan University, Taiwan. From 1996 to 1999, he was an assistant professor at the Mechanical Engineering and Applied Mechanics Department at the University of Michigan, Ann Arbor. In 1999, he joined the University of California at Berkeley and is now an associate professor at Mechanical Engineering Department and co-director at Berkeley Sensor and Actuator Center, NSF/Industry/University research cooperative center. His research interests are in design, modeling, and fabrication of microstructures, microsensors, and microactuators as well as mechanical issues in microelectromechanical systems including heat transfer, solid/fluid mechanics, and dynamics. He holds eight US patents in the area of MEMS. Dr. Lin is the recipient of the 1998 NSF CAREER Award for research in MEMS Packaging and the 1999 ASME Journal of Heat Transfer Best Paper Award for his work on microscale bubble formation. He served as chairman of the Micromechanical Systems Panel of the ASME Dynamic Systems and Control Division in 1997 and 1998 and led the effort in establishing the MEMS subdivision in ASME and is currently the vice chairman of the Executive Committee.